Numerical simulation of the self-propelled performance of container ships based on CFD

Qianqian Li [1, a], Binlin Zhao [1, b], Jialin Wang [1, c, *], Xueyuan Jing [1, d], Chenyun Yao [1, e], Yuting Zhang [1, f]

[1] School of Naval Architecture and Ocean Engineering, Jiangsu University of Science and Technology, Zhenjiang 212100, China.

[a] 3240300871@qq.com, [b] 3156597771@qq.com, [c, *] 349910872@qq.com, [d] 1751157803@qq.com, [e] 2406372010@qq.com, [f] 2086900199@qq.com

Abstract. In order to analyse the self-propelled performance of 98TEU inland container ships, this paper adopts the CFD method to numerically simulate the self-propelled performance of the ship based on STAR-CCM+. This paper adopts the method of fixed speed and variable rotation speed, by adjusting the rotation speed so that the thrust generated by the propeller can overcome the resistance. CFD technology is used to simulate the ship drag, propeller thrust and other parameters generated when the ship sails on its own, and based on the simulation results, a real-vessel speed prediction curve is established to obtain the ship's target speed under the power of the main engine. The research results show that the CFD method can accurately simulate the self-sailing of the ship, and the method provides a reference for the self-sailing performance evaluation of similar ships.

Keywords: 98TEU inland container ship; CFD method; self-propelled.

1. Introduction

With the continuous development of inland water transport traffic, the performance optimisation, energy saving and emission reduction of inland river container ships, as an important tool for water transport, has become a focus of attention for the shipping industry. Traditionally, the evaluation of ship performance mainly relies on model tests and real ship tests, but these methods are often time-consuming and costly. In recent years, Computational Fluid Dynamics (CFD) technology, with its advantages of low cost, short time consumption, and high accuracy, provides a new way for ship design and performance evaluation.

Ship model self-sailing test can obtain the interaction factors between the propeller and the hull such as companion flow fraction, thrust derating fraction and other interaction coefficients, which is an important means to analyse and study the components of propulsive efficiency [1]. Many scholars have already used CFD techniques to analyse the relevant characteristics of ships. Carrica [2] et al. investigated the self-propelled calculation of KCS ship model with sail and oar with free lift and longitudinal inclination under hydrostatic water based on the overlapping dynamic mesh technique; Yang Chunlei and Zhu Renchuan [3] et al. applied Computational Fluid Dynamics (CFD) methods to investigate the unsteady viscous flow field of the KCS container ship with oars and the KVLCC2 with oars and rudder. The numerical simulation of the unsteady viscous flow field of an oil tanker was carried out; Liu Xiangjun and Sun Cunlou [4] also considered the free liquid surface, the rotational motion of the real propeller, and the numerical computation of the overall flow field of the ship/propeller was achieved in the numerical pool.

This paper takes the 98TEU inland container ship as the research object, and numerically simulates its self-hauling performance based on the CFD software STAR-CCM+, adopting the method of fixed speed and variable rotation speed, so that the thrust generated by the propeller can overcome the resistance of the hull. According to the numerical simulation results obtained from the real ship speed prediction curve and experimental values for comparison, it can be seen that the CFD method can accurately simulate the ship's self-hauling, for the self-hauling performance evaluation of similar ships to provide a reference value.

2. CFD basic theory and numerical methods

2.1 Basic Theory

CFD software is widely used in the field of ship and ocean engineering for numerical simulation and analysis of ship hydrodynamic performance, which has the advantages of low cost, short time consumption, and can well deal with model scale effects. The CFD-based solution process is mainly divided into several steps as shown in Figure 1.

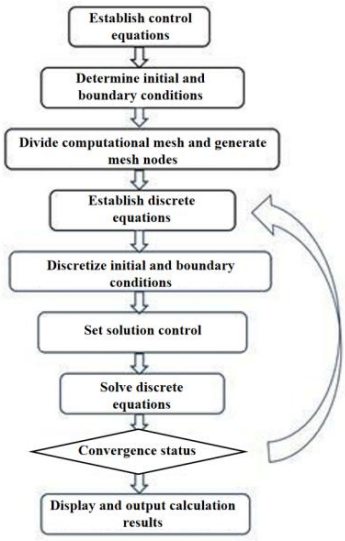

Fig. 1 CFD calculation flowchart

2.2 Numerical methods

When analysing the flow of an incompressible viscous fluid, the basic principles of conservation of mass and conservation of momentum must be satisfied. Therefore, the governing equations chosen include the continuity equation (mass conservation equation) and the Navier-Stokes equation (momentum conservation equation).

(1) The continuity equation

$$\frac{D\rho}{Dt} + \rho div(v) = 0 \#(1)$$

In this equation, ρ is the fluid density and v is the velocity vector of the flow field.

(2) Momentum conservation equation (Navier-Stokes)

For viscous fluid motion, when the viscosity is a constant, there is the N-S equation

$$\rho\frac{Dv}{Dt} = \rho F_b - gradp + div(2\mu S) + \frac{2}{3}grad(\mu divv) \#(2)$$

In this equation, μ represents the dynamic viscous coefficient, F_b indicates the body force, p denotes the pressure, and S signifies the strain rate tensor. The left side of the equation describes the inertial force per unit volume of the fluid. The first term on the right corresponds to the mass force per unit volume; the second term reflects the pressure gradient force acting on the fluid per unit volume; the third term accounts for viscous deformation stress, and the fourth term represents the expansion stress of the viscous body.

(3) Standard $k-\omega$ model:

The standard $k-\omega$ model has wide applicability and relative accuracy in numerical simulations, thus becoming the main turbulence model in fluid dynamics calculations. The transport equation for turbulent kinetic energy is given below:

$$\frac{\partial(\rho k)}{\partial t} + \frac{\partial(\rho k u_i)}{\partial x_i} = \frac{\partial}{\partial x_j}\left[\left(u + \frac{u_t}{\sigma_k}\right)\frac{\partial_k}{\partial x_j}\right] + G_k + G_b - p\varepsilon - Y_M + S_k \#(3)$$

Where k is defined as:

$$k = \frac{1}{2} u_j u_i \#(4)$$

3. Numerical model and meshing

3.1 Modelling

This project is a 98TEU inland container ship, in order to improve the calculation efficiency and make a direct comparison with the test results, the scaled-down model is used to carry out numerical modelling and calculations, the scaling ratio is 1:8, and the table of comparison parameters of the 3D model for CFD calculations is shown in Table 1.

Table 1. Comparison parameters of CFD computed 3D models

serial number	sports event	actual value	modelled value	relative error
1	Waterline length (L_{WL})	68.0m	8.5m	0 per cent
2	Type width (B)	12.7m	1.588m	0 per cent
3	Type depth (Z)	3.9m	0.488m	0 per cent
4	Bow draught (T_F)	2.2m	0.275m	0 per cent
5	Transom draft (T_a)	2.2m	0.275m	0 per cent
6	Drainage volume of type (▽)	1593.027	4.08	0 per cent
7	Wet surface area (S_W)	1025.7m^2	16.02m^2	0 per cent
8	Longitudinal Center of Buoyancy (%L_{PP})	0	0	0 per cent
9	Centre of buoyancy vertical position VCB (height from baseline)	1.155m	0.185m	0 per cent

In order to standardise the simulation process, the following points are made about the coordinate positions of the simulation model imported into STAR-CCM+:

1) The origin of the simulation coordinate system is the same as the CAD file.
2) X-axis pointing towards the bow
3) Y-axis towards the port side
4) Z-axis is vertically upwards

The following is a comparative view of the 3D model in different orientations, as shown in Figure 2.

(a) Main view (b) Top view

Fig. 2 Comparative view of ship modelling with different orientations

3.2 Computational domain and meshing

This paper covers a total of five different speed points, namely 0.982m/s, 1.081m/s, 1.178m/s, 1.277m/s, 1.376m/s. The initial setting of the simulation is that the ship is kept stationary, and the water velocity is given to flow at speeds ranging from 0.982m/s to 1.376m/s, and the simulation strategy of fixing the speed and adjusting the rotational speed is adopted to explore the ship's performance under different working conditions.

This simulation adopts a square computational domain to numerically simulate and analyse the self-propelled performance of the ship, and the computational domain is divided as follows: the bow is 3.5L_{wl} away from the inlet of the computational domain, the stern is 1.5L_{wl} away from the

outlet, and there are a total of $6L_{wl}$ in the length direction; there are a total of $1.5L_{wl}$ in the breadth direction of the computational domain; and the height direction of the computational domain is taken as $0.5L_{wl}$ above the waterline, and $1.5L_{wl}$ below the waterline. The boundary surface of the computational domain is taken to be divided by angles, the inlet surface and top of the computational domain are defined as velocity inlet and the outlet is defined as pressure outlet boundary. Since the constructed 98TEU inland container ship is a symmetric model, the plane where the longitudinal section is located in the hull is defined as the symmetric plane, and the rest are set as wall planes. The final established computational domain and boundary conditions are shown in Fig. 3:

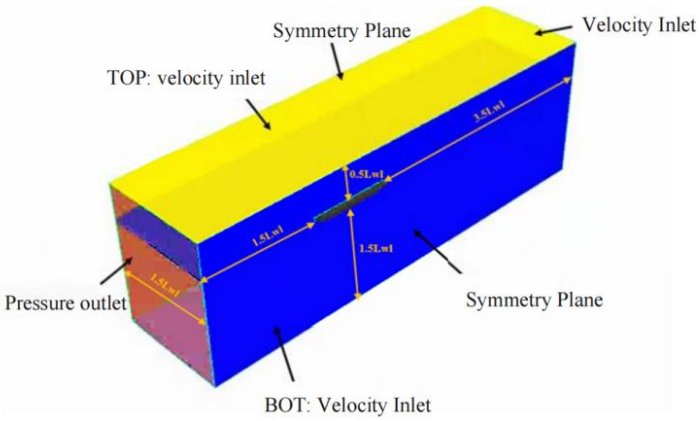

Fig. 3 Computational domain and boundary conditions

The grid of the computational domain is mainly divided into peripheral basin grid and ship encrypted area grid, using the cut body grid cell generator, and local encryption of the ship hull and near the waterline surface, to get the total grid of the computational domain is about 3.78 million, the critical part of the ship's hull grid, the grid of the encrypted place of the free liquid surface and the encrypted grid of the Kelvin wave are shown in Fig. 4, Fig. 5 and Fig. 6 below.

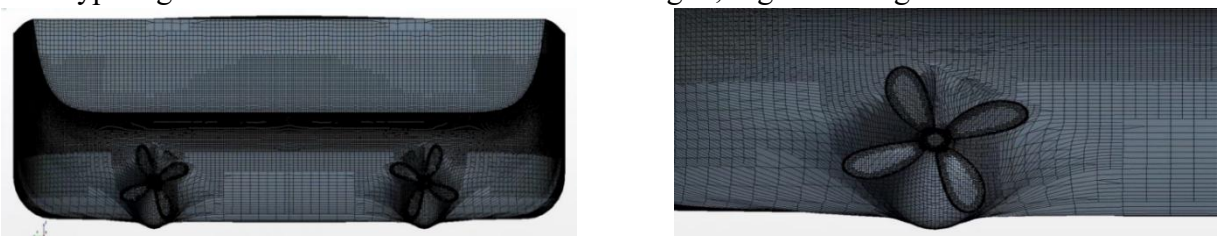

(a) Stern seal plate grid encryption (b) Propeller grid encryption

Fig. 4 Schematic diagram of the mesh of the key parts of the hull

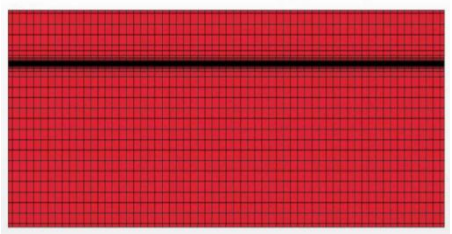

Fig. 5 Grid at free level encryption

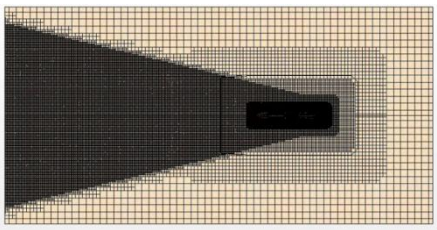

Fig. 6 Kelvin wave encryption grid

3.3 Grid quality verification

For the simulation software STAR-CCM+, the computational target body is generally divided into several small volumes by dividing the mesh, and the quality of these meshes is crucial to

determine whether the computation can go on smoothly. Therefore, mesh quality verification is required. The current ways of evaluating the grid quality in STAR-CCM+ include grid volume variation, face validity of the grid, grid cell skew angle, etc. In this subsection, the three methods will be used to verify that the grid quality of the numerical simulation in this paper is good and the results of the numerical simulation are reliable. The three validation methods are shown in Fig. 7, Fig. 8 and Fig. 9.

Fig. 7 Grid Volume Change

Fig. 8 Face validity of the grid

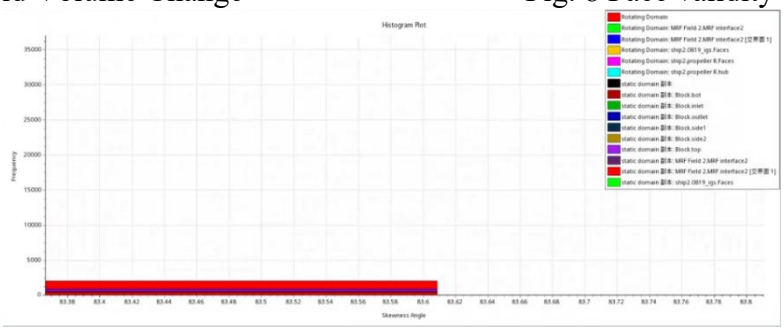

Fig. 9 Mesh Skew Angle

The number of grids in the computational domain of this paper is 3.78 million grids, according to the analysis of the above Fig. 7, Fig. 8 and Fig. 9, it can be seen that the minimum volume change is greater than 1e-3, and the ratio is close to 1; the face validity is greater than 0.9; the grid deflection angle is 83.61°, which is less than 85°, therefore, the range of the grid volume change, the grid face validity, and the grid deflection angle are all in line with the standard, then the mesh quality of this paper's numerical simulation is good.

4. Ship self-propelled Performance analysis

4.1 Propeller open water performance

This simulation calculates the open water performance of the model paddle at J=0.038~0.770 and takes the average value of the thrust coefficient and torque coefficient in one rotation cycle of the calculation results for the current working condition. In this paper, the SST k- ω turbulence model is chosen for the calculation, which takes into account the transport characteristics of turbulent shear and is more suitable for the simulation of the complex flow field around the surface paddle.

Based on the data calculated by CFD, the propeller open water behaviour curve and the propeller open water behaviour versus load curve are plotted in Figures 10 and 11 below.

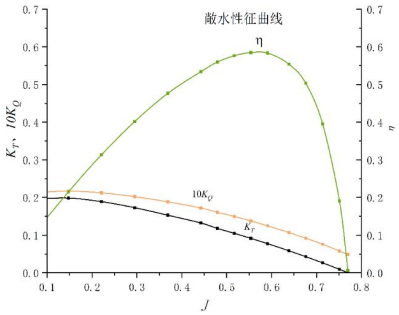

Fig. 10 Open water characterisation curve

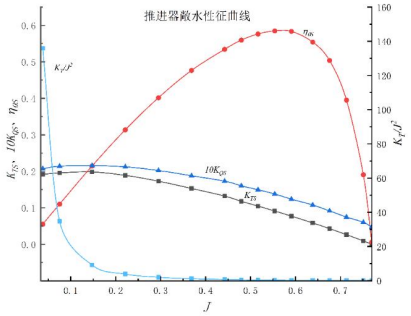

Fig. 11 Open Water Characteristics and Load Curves

4.2 Ship resistance calculation

According to 3.3.2 of CCS "Guidelines for the speed and power assessment of inland waterway vessels based on Computational Fluid Dynamics (CFD)", the interval between the speed points for drag calculation should be not less than 1km/h, and the speed points of the effective power curves should be not less than 5. Therefore, there are 5 different speed conditions in the simulation, and the drag and speed power conversions obtained from the numerical simulation of the ship according to the CFD are as follows: Table 2. As shown in Table 2, this paper adopts the three-factor method to convert the resistance between the ship model and the real ship.

Table 2. Calculation of resistance conversion for live ship

sports event	Vm (m/s)	Vs (km/h)	Rtm (kg)	Rts(KN)	Pes (KW)	Fr	FD (kg)
1	0.982	10.000	3.060	22.537	62.608	0.109	0.624
2	1.081	11.000	3.646	26.693	81.575	0.120	0.643
3	1.178	12.000	4.359	31.621	105.392	0.131	0.840
4	1.277	13.000	5.203	36.909	133.290	0.142	0.922
5	1.376	14.000	6.185	41.674	158.778	0.153	0.999

Based on the contents of the above table, the resistance and effective power of the real vessel are plotted as shown in Figures 12 and 13 below:

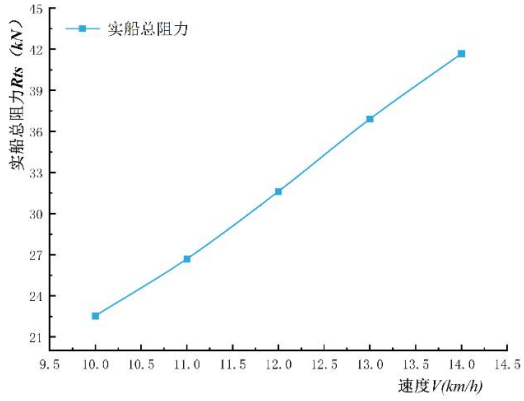

Fig. 12 Total resistance curve of the real vessel

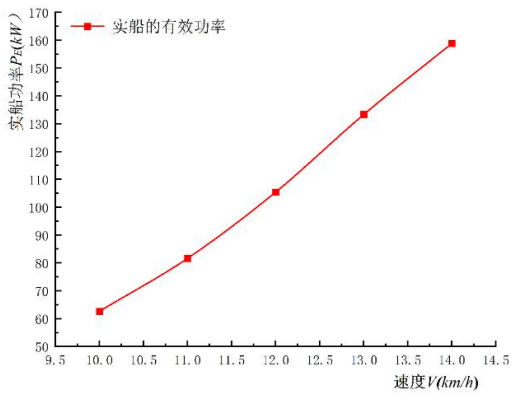

Fig. 13 Effective power curve of the real vessel

4.3 Simulation results of ship self-propelled experiment

In this section, the self-sailing factor of 96TEU inland waterway container ships at different speeds is investigated. In order to accurately simulate the actual sailing condition of the ship and strictly comply with the speed power specification, this paper adopts the method of fixed speed and variable rotational speed to carry out numerical simulation calculations. The rotational speed of the propeller is adjusted to make the thrust emitted by the propeller just able to overcome the drag force

(Rm-FD), and the speed for the design condition of this ship are 0.982m/s,1.081m/s, 1.178m/s, 1.277m/s and 1.376m/s. The rotational speeds for each speed condition are shown in Table 3 below:

Table 3. Working conditions for each speed

Vm (m/s)	Speed (rps)			
0.982	5.940	7.140	8.140	9.140
1.081	7.140	8.140	9.140	10.940
1.178	8.140	9.140	10.940	12.230
1.277	9.140	10.940	12.230	13.300
1.376	10.940	12.230	13.300	13.780

Numerical simulation is more, this paper only shows the self-propelled waveform graphs, self-propelled Y+ on hull with different rotational speeds at 0.982m/s airspeed, as shown in Fig. 14 and Fig. 15 below:

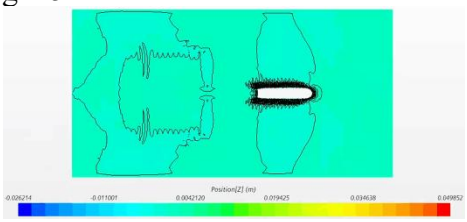

(a) 5.94 rps

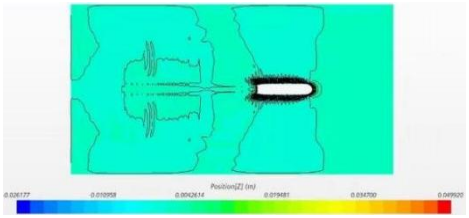

(b) 7.14rps

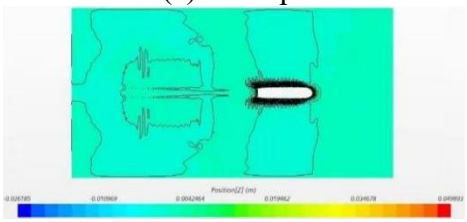

(c) 8.14 rps

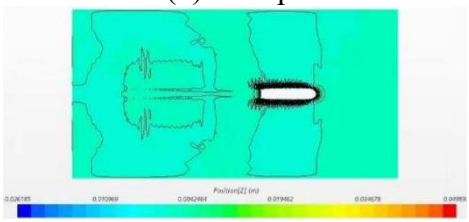

(d) 9.14 rps

Fig. 14 Waveforms at different rotational speeds at 0.982m/s

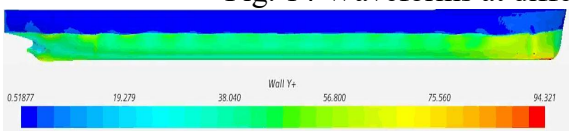

(a) 5.94 rps

(b) 7.14rps

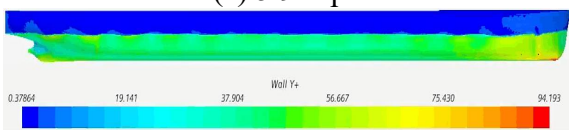

(c) 8.14 rps

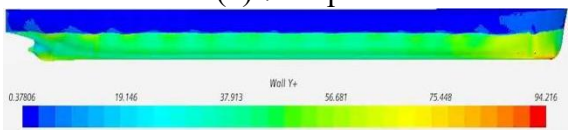

(d) 9.14 rps

Fig. 15 Y+ plots for different rotational speeds at 0.982m/s

According to the numerical simulation results to draw the self-sailing test curve, interpolation to obtain the real ship self-sailing point data as shown in Figure 16 below.

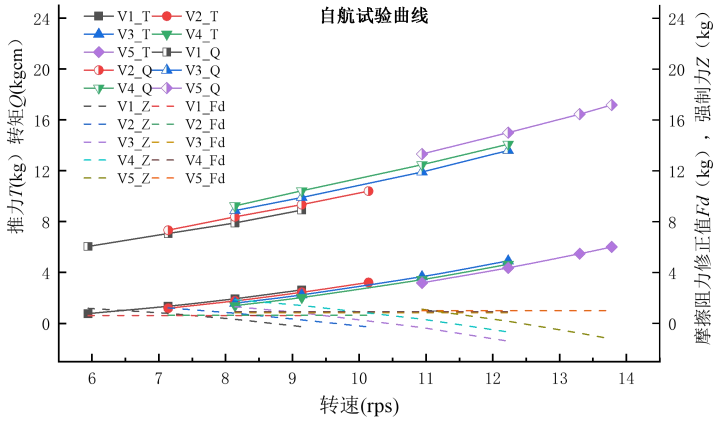

Fig. 16 Curves of real ship self-propelled test

From the image analysis, it can be seen that the faster the rotational speed of the propeller produces more thrust and torque at the same speed condition. The curve of the friction resistance correction value is relatively smooth and does not show large fluctuations. As for the forcing force, it shows a small decrease with the increase in speed. The greater the speed, the greater the thrust, torque and forcing force generated by the ship, which provides strong data support for further investigation of the ship's self-propelled performance.

4.4 Calculation of self-hauling factor for real ships

The self-sailing factor is an important parameter to judge the excellent propulsion performance of a ship, reflecting the interaction between the hull, propeller and main engine. The self-sailing factors usually include thrust derating fraction (t), companion flow fraction (ω), relative rotational efficiency (η R), hull efficiency (η H) and propulsive efficiency (η D).

According to the calculation of the ship principle formula, the shape factor of this paper's numerical simulation is 1.182, the roughness allowance is Z\Q=0.7336×10-3, and the self-hauling factor of the real ship obtained by converting the real results of the CFD ship simulation is shown in Table 4 below.

Table 4. Calculation of self-hauling factor for real ships

Shape factor (1+k): 1.182		Roughness allowance Z\Q=0.7336×10^{-3}				
Speed of the live ship	Vs(kn)	5.3996	5.9395	6.4795	7.0194	7.5594
The friction resistance coefficient of the corresponding ship mould	Cfm ×10^3	3.1042	3.0521	3.0066	2.9649	2.9271
The corresponding friction resistance coefficient of the real ship	Cfs ×10^3	1.9077	1.8828	1.8605	1.8403	1.8269
Real Ship Thrust Reduction Score	t_s=t_m	0.2274	0.2507	0.2278	0.2150	0.2390
Relative rotational efficiency of real ships	η_{Rm}	1.1900	1.2785	1.3218	1.3346	1.3972
live-aboard companionway fraction (LBSF)	ω_m	0.2607	0.2466	0.2390	0.2349	0.2149

4.5 Sailing characteristics of the real vessel

Based on the CFD numerical simulation results derived above the real ship speed prediction curves are plotted as shown in Figure 17 below and the speeds of the actual propellers are evaluated in ballast draught and four main engine states as shown in Table 5 below.

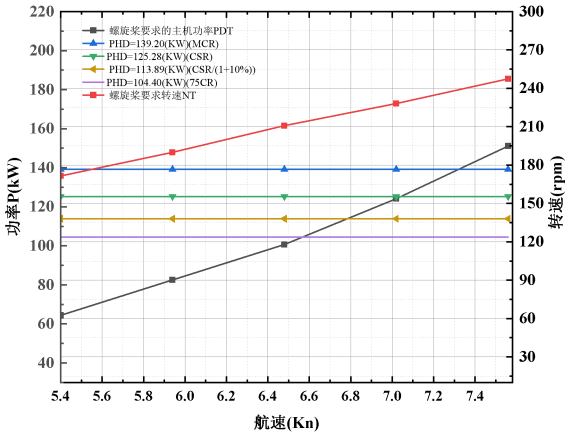

Fig. 17 Plot of the predicted speed of a live vessel

Table 5. Estimated Speed Table

draught	host state	Power received (kW)	Estimated speed (m/s)	Estimated speed (Kn)	Propeller speed (rpm)
Ballast draft (2.2m/2.8m)	MCR	145×0.96 = 139.200	3.7658	7.3201	238.848
	CSR	145×0.9×0.96 = 125.280	3.6230	7.0426	228.947
	75%MCR	145×0.75×0.96 = 104.400	3.3727	6.5660	213.467
	CSR/(1+10%)	145×0.9×0.96/1.1 = 113.890	3.4880	6.7801	220.440

The target speed in this paper is 13km/h, which is about 3.611m/s. According to the above table, the analysis shows that the ship can reach the target speed under MCR and CSR main engine state. However, under 75% MCR and CSR/(1+10%) main engine condition, the predicted speed is lower than the target speed. Therefore, it is recommended that the ship should be operated under MCR or CSR main engine condition, and for 75% MCR and CSR/(1+10%) main engine condition, optimisation of the hull line or propulsion system can be considered to improve the speed and energy efficiency.

5. Summary

In this paper, the self-propelled performance of a 98TEU inland container ship is numerically simulated using computational fluid dynamics (CFD) technology. Through the three-dimensional geometric model of the ship hull, the calculation of domain grid division based on the flow field characteristics, and the setting of reasonable boundary conditions, the self-propelled characteristics of the ship at different speeds are successfully simulated by using the method of constant speed and variable rotation speed. Under the main engine power, the estimated speed obtained by CFD numerical simulation can reach the target speed, and the propeller can provide enough thrust under the design condition, which is in good agreement with the experimental data, so the CFD method can accurately simulate the self-propulsion of the ship, and it also provides a reference for the subsequent evaluation of self-propulsion performance or optimisation of the propulsion system of other types of ships.

References

[1] Liu Xiangjun, Sun Cunlou. Research on the self-propelled test method of numerical pool ship model[J]. Ship Science and Technology,2011,33(02):28-31.

[2] Carrica P M, Castro A M, Stern F . Self-propulsion computations using a speed controller and a discretized propeller with dynamic overset grids[J]. Mar Sci Technol,2010, 15(4):316-330.DOI:10.1007/s00773-010-00 98-6

[3] YANG Chunlei, ZHU Renchuan, MU Guoping, et al. Numerical simulation of boat/paddle/rudder interference based on CFD method[J]. Hydrodynamics Research and Progress Series A,2011, 26(06):667-673.

[4] Liu Xiangjun, Sun Cunlou. Research on the self-propelled test method of numerical pool ship model[J]. Ship Science and Technology,2011,33(02):28-31.